CARBON 48 (2010) 4535–4541

available at www.sciencedirect.com

ScienceDirect

journal homepage: www.elsevier.com/locate/carbon

# Preparation of high purity helical carbon nanofibers by the catalytic decomposition of acetylene and their growth mechanism

*Xian Jian* [a], *Man Jiang* [a], *Zuowan Zhou* [a,*], *Mingli Yang* [b,**], *Jun Lu* [a], *Shuchun Hu* [a], *Yong Wang* [a], *David Hui* [c]

[a] *Key Laboratory of Advanced Technologies of Materials (Ministry of Education), School of Materials Science and Engineering, Southwest Jiaotong University, Chengdu, Sichuan 610031, China*

[b] *Institute of Atomic and Molecular Physics, Sichuan University, Chengdu 610065, China*

[c] *Department of Mechanical Engineering, University of New Orleans, New Orleans, LA 70148, USA*

ARTICLE INFO

*Article history:*
Received 10 February 2010
Accepted 15 August 2010
Available online 19 August 2010

ABSTRACT

Helical nanofibers were synthesized at 271 °C using acetylene gas as the reactant and copper nanocrystals, produced by decomposition of copper tartrate, as the catalyst. Their chemical structure was confirmed to be organic compounds containing C=C groups using characterization by FT-IR, $^{1}$H NMR and elemental analyses. The morphologies of the catalyst before, during and after the fiber growth were observed by SEM and TEM, and the results reveal that the shape of the copper nanoparticles changes from quasi-spherical to polyhedral during the adsorption of acetylene. Chemisorption of acetylene on different planes of the copper crystal was simulated by density functional theory calculations under the generalized gradient approximation. The adsorption energy on the (1 1 1), (1 0 0) and (1 1 0) planes of Cu was investigated to address the interaction modes between acetylene and Cu surfaces. The adsorbability is in the order (1 0 0) > (1 1 1) > (1 1 0). Based on the experimental and theoretical evidence, a growth mechanism of coordination polymerization and asymmetric growth on distinctive crystal planes was proposed to interpret the structural and morphological variations of the nanofibers.



## 1. Introduction

The study of carbon helical materials such as micro-coils and nano-coils has received increasing attention in recent years [1,2]. Davis et al. [1] are the first to report the vapor growth of thin carbon fibers twisted together in the form of a rope. However, the growth of such coiled fibers from the vapor phase is extremely accidental and poorly repeatable. Motojima et al. [3–5] have found that regular micro-coiled fibers could be obtained with high reproducibility by the catalytic pyrolysis of acetylene with a small amount of sulfur or phosphorus impurity. The helical fibers are mostly obtained by chemical vapor deposition (CVD) on transition-metal catalysts of iron [3], nickel [4,5], titanium [6] and their alloys [7,8]. In general, they are prepared by high-temperature (>500 °C) catalytic decomposition of organic gas such as acetylene or benzene. The coiled fibers are chiral with a three dimensional helical/spiral morphology and possess unique characteristics, such as super-elasticity [3,4,9], wide band absorption of electromagnetic waves [10,11], hydrogen absorption [12] and so on. These

* *Corresponding author:* Fax: +86 28 8760 0454.
** *Corresponding author:*
E-mail addresses: zwzhou@at-c.net (Z. Zhou), myang@scu.edu.cn (M. Yang).
0008-6223/$ - see front matter © 2010 Elsevier Ltd. All rights reserved.
doi:10.1016/j.carbon.2010.08.035

unique properties make coiled fibers a very appealing material for potential applications.

In the last few years, Qin et al. [13,14] investigated the growth condition of helical nanofibers over copper nanoparticles and found that coiled carbon nanofibers could be obtained after heat treatment at >900 °C. Regular helical nanofibers with a symmetric growth mode could be prepared by the decomposition of acetylene using copper nanocrystals as catalyst without any other catalytic additive. The reaction proceeds at relatively low temperature without toxic chemicals, which is of great significance in energy saving and environmental protection. Besides, the symmetric morphology of the obtained helical nanofibers may greatly enrich their potential applications in functional materials.

The growth mechanism of CVD-grown carbon fibers or carbon nanotubes is known as the vapor–liquid–solid growth mode [15,16], that is, the liquid catalyst droplets absorb the building-block material from the surrounding vapor, and then deposits carbon on their interfaces. However, this mechanism can hardly be applied in the growth of the helical fibers prepared by Qin et al. [13,14]. In fact, some hints of a new growth mechanism can be obtained by analyzing the details of the catalyst particles and the nanofibers. The morphology and properties of the nanofiber depend closely on the composition, size, and morphology of the catalyst. The prepared nanofiber can be straight or helical by tuning the shape and the size of Cu nanoparticles. It would be meaningful to study how the Cu nanoparticles change their morphologies and catalyze the formation of the helical nanofibers. In this work, the helical nanofibers were synthesized under the catalysis of Cu nanoparticles, and their structures were characterized with SEM, FT-IR, $^1$H NMR, etc. In addition, the adsorption of acetylene on the Cu planes was simulated with density functional theory (DFT) calculations to address the surface effect on the reactions. A coordination polymerization mechanism and asymmetric growth on distinctive crystal planes were then suggested based on the experimental and computational evidences.

## 2. Experimental procedures

### 2.1. Synthesis of the samples

As a catalyst precursor, copper(II) tartrate was prepared by a precipitation method [14]. The preparation of the nanofibers was carried out at atmospheric pressure in a quartz tube with 45 mm in diameter and 1300 mm in length. The quartz tube was set into the horizontal furnace and heated at certain heating rate. A ceramic boat paved with a layer of the catalyst precursor was placed into the reaction tube. The heating continued until the catalyst precursor was decomposed into copper particles. Acetylene was then induced into the tube and decomposed to produce the nanofibers. Fast heating (>3 °C/min) under the protection of argon favors the formation of straight nanofibers, while slow heating (<3 °C/min) without argon favors helical nanofibers.

### 2.2. Characterizations of the samples

Thermogravimetric (TG) measurement was performed using a Germanic thermoanalyzers STA 449C Jupiter under nitrogen atmosphere at the heating rate of 10 °C/min. The morphologies of the catalyst precursor and the catalyst particles were observed by means of environmental scanning electronic microscope (ESEM, Fei, Quanta 200) with an accerlerating voltage of 20.0 kV and transmission electron microscopy (TEM, H-700H) at an accerlerating voltage of 160 kV. The crystal structure of catalyst particles was investigated using X-ray diffraction (XRD, Panalytical X'Pert PRO diffractometer with Ni-filtered, the Netherlands). The chemical constituents of the helical fibers were confirmed through FT-IR analysis (Nicolet 5700, USA) from 4000 to 400 $cm^{-1}$ at a resolution of 4 $cm^{-1}$ and $^1$H NMR spectra (Bruker AV II-400 MHz) at the room temperature with tetramethylsilane (TMS) as the internal standard. Besides, the C/H molar ratio was measured by elemental analysis (Carlo Erba 1106).

## 3. Results and discussion

### 3.1. Analyses of the catalyst and the nanofiber

The TG analysis was used to ascertain the decomposition condition of the catalyst precursor, and the results reveal that it decomposes from 270.9 to 366.9 °C. A fine powder was obtained after the catalyst precursor was heated to 271 °C for 30 min under argon atmosphere. Fig. 1a gives the TEM image of the decomposed powder. These fine particles exhibit irregular shapes with an average grain size of about 50 nm. Fig. 1b shows the TEM image of the typical morphology of the catalyst embedded in the helical nanofibers after reaction at 271 °C. It can be found that the grain sizes of the catalysts are close to those of the particles decomposed from the precursor (Fig. 1a), but their shapes change from quasi-spheres with smooth surface to polyhedral crystals with distinctly sharp edges. In the XRD profile (Fig. 1c), the three characteristic diffraction peaks of metallic copper over 40° are clearly observed, which agrees well with the standard copper diffraction pattern (ICDD, PDF file No. 03-065-9743). A broad peak in the range of angle below 40° is assigned to the amorphous structure of the helical nanofibers. No diffraction peak of other metallic impurity is noted in the experiments, and the average grain size of the catalyst particle is estimated about 33 nm by the Scherrer formula using the full width at half maximum value of the XRD diffraction peaks. So the polyhedral substance locating in the middle of the nanofiber should be assigned to copper nanocrystal. The copper tartrate decomposes into copper particles before the nanofiber forms, but the particle shapes start to change from spherical to polyhedral when the helical nanofiber forms and grows up. Therefore, it is polyhedral copper nanoparticle that is responsible for the growth of the helical nanofiber.

The growing process of the fiber was investigated in terms of its morphology evolution so as to establish its correlation with the morphology of the catalyst particles. At the initial stage, the acetylene is adsorbed on the surface of the Cu nanoparticles, as shown in Fig. 2a. Some of the particles are induced to form into polyhedron; the typical geometric shape is shown in the inset of Fig. 2a. As the reaction proceeds, the nanofibers start to grow on the surface of the particle. The formed nanofibers appear to be straight at the early stage, which should in fact be viewed as "straight nanofiber". Most

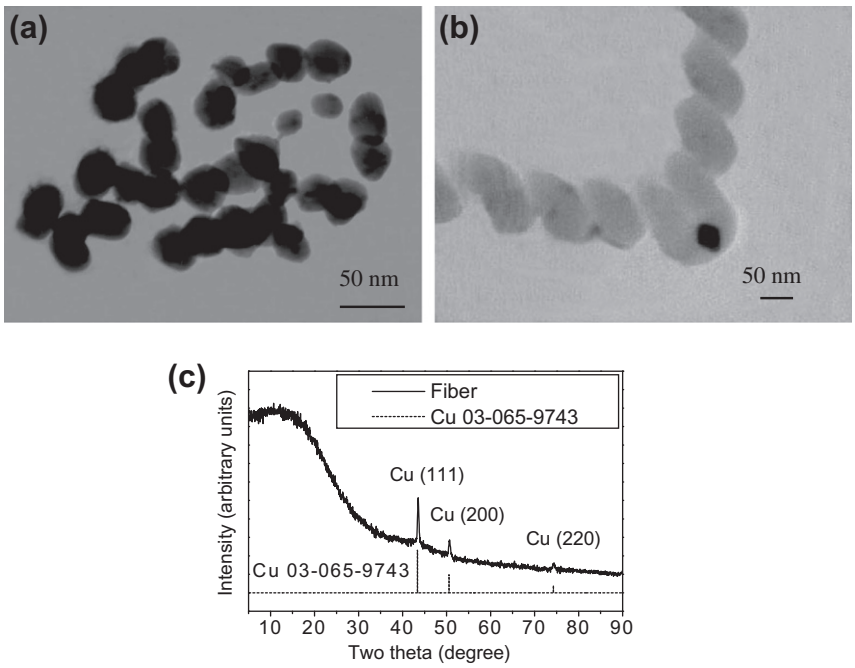


**Fig. 1 – (a) TEM image of the catalyst prepared using copper tartrate catalyst precursor under argon at 271 °C, (b) TEM image of the helical nanofibers obtained at 271 °C, and (c) XRD pattern of the helical nanofibers obtained at 271 °C.**

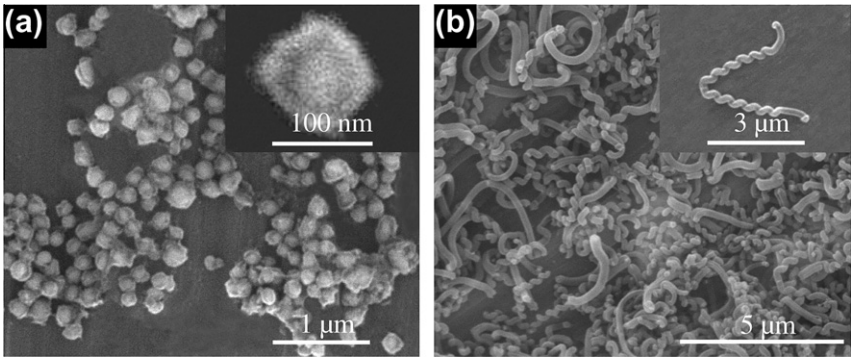


**Fig. 2 – SEM images of the samples at different growth stages: (a) 5 min and (b) 15 min. The typical shape change of the catalyst particle is shown in the inset of Fig. 2a, and the inset of Fig. 2b exhibits the typical symmetric style of the sample (b).**

of the nanofibers grow in the form of helical structure when the reaction time is up to 15 min. The typical morphology change of the nanofiber is shown in the inset of Fig. 2b, in which the twin fibers symmetrically grow on a Cu nanoparticle in identical shape, diameter and number of the helixes.

The conditions of heating stage are found to be closely dependent on the morphology of the catalyst particle, which finally determines the different morphologies of the nanofibers. The helical fibers with regular coils (Fig. 3a) are obtained under several conditions: the heating rate is less than 3 °C/min, the atmosphere for decomposition of the catalyst precursor is acetylene, and the reaction temperature is between 195 °C and 271 °C. In contrast, the straight fibers (Fig. 3b) are obtained if the heating rate for the catalyst precursor increases up to 3 °C/min under argon atmosphere. The Cu particles located in the center of the straight fiber are mostly ellipsoids and their sizes are often larger than 100 nm. Thus we speculate that the catalyst anisotropy of the copper particles disappears as the Cu particles become bigger in size, leading to the formation of straight nanofibers.

### 3.2. *Chemical structure*

Fig. 4 shows a typical FT-IR spectrum of the nanofibers prepared at 271 °C, in which the peaks at 2926.3, 2870.6, and 1451.8 $cm^{-1}$ are ascribed to the C–H vibration in $CH_2$, the peak at 1601.3 $cm^{-1}$ is assigned to C=C stretching vibration, the peaks at 3018.8 and 1030.0 $cm^{-1}$ are resulted from C–H stretching and deformation in C=C, respectively, and the C–H deformation in $CH_3$ induces the peak at 1375.7 $cm^{-1}$.

The IR analysis reveals that the chemical structure of the nanofibers contains both C=C and saturated $CH_2$, $CH_3$ groups. The OH group associating to 3447.8 $cm^{-1}$ may arise from the oxidation in air, which is consistent with the mechanism of traditional polyacetylene oxidation [17]. Elementary analysis reveals that the C/H molar ratios of the prepared coiled fibers

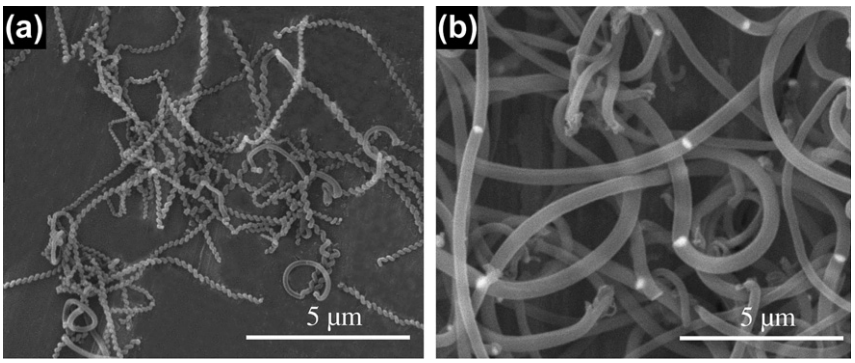


**Fig. 3 – SEM images of two kinds of nanofibers prepared at 271 °C using catalysts generated from different heating atmosphere and heating rate: (a) helical nanofiber with catalyst under acetylene at low heating rate (<3 °C), (b) straight nanofiber by catalyst under argon at high heating rate (>3 °C).**

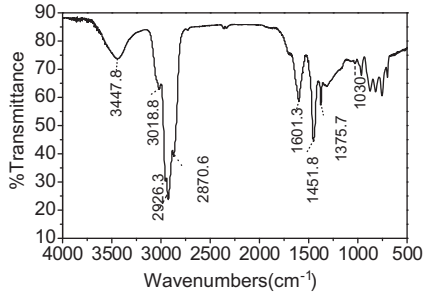


**Fig. 4 – Typical FT-IR spectrum of the helical nanofibers prepared at 271 °C.**

are 1.139 at 200 °C, 1.210 at 250 °C and 1.252 at 300 °C. $^1$H NMR spectrum of the fiber prepared at 271 °C also confirms that unsaturated groups exist in the fibers. There are two peaks at 2.086 induced by =C–$CH_3$ group and 3.385 by =C–OH. The molar ratio of saturated groups is 19% calculated from the area ratio. These results confirm the existence of the unsaturated groups and their oxides that formed in air. Thus we suggest that the nanofiber is a kind of organic compound comprising C=C group with minor oxidization.

### 3.3. *Polymerization process of the nanofiber*

Based on the above results of elemental analysis, IR and $^1$H NMR, the as-prepared nanofibers belong to a new organic compounds containing C=C group. The strong interaction between acetylene and Cu crystal surface is one of the most possible reasons that result in the formation of the nanofibers, as revealed from the results of SEM in the Fig. 2a. We are thus interested in the interaction mode between acetylene and Cu surface.

The adsorption of gas such as acetylene on single-crystal surfaces under ultrahigh-vacuum (UHV) conditions has been an active field for a long time [18–23]. In fact, the acetylene trimerization was studied under UHV conditions on a variety of metallic single-crystal surfaces such as Pd(1 1 1) [18,19], Cu(1 1 0) [20,21], Cu(1 0 0) [22], Cu(1 1 1) [23]. Qin et al. [14,24] studied the reactions of acetylene on Cu nanocrystal at temperature ranging from 195 to 400 °C and speculated that the deposition reaction is carried out simultaneously in two paths, coupling (94%) and decomposition (6%) at 195 °C.

In the light of our experimental observations and theoretical simulations in the later section, the adsorption of acetylene on Cu surface and the interaction between the acetylene and the copper play key roles in forming the helical carbon nanofibers. The helical organic nanofiber is formed according to coordination polymerization, as illustrated in Fig. 5. At the initial stage, when acetylene is adsorbed on the copper surface, the interactions occur between the unoccupied orbital of the Cu atom and the $\pi$ electron of the acetylene molecule, leading to the formation of a coordination bond. After that, the coordinate bond develops gradually into a covalent bond through electron rearrangement, and an unoccupied orbital is regenerated for the next process, which is analogous with the coordination polymerization.

In addition to the acetylene polymerization, the acetylene decomposition also occurs and leads to the deposition of a small amount of carbon and the formation of hydrogen [24]. Then this kind of organic fiber contains a small amount of saturated groups, such as $CH_2$ and $CH_3$, due to additional reaction of some hydrogen. With regard to the saturated groups, we speculate some reduction by hydrogen and chain-branching reaction may occur during the polymerization process.

### 3.4. *First-principles study of acetylene adsorption on the Cu surfaces*

In order to reveal the impetus for the shape change, it is necessary to investigate the variation of the surface properties upon acetylene adsorption, in particular to the variation of surface energy, which is directly related to the particle shapes. However, the surface energy of crystalline metal and semiconductor can hardly be measured. We studied the chemisorptions of acetylene on the crystal planes of Cu(1 0 0), (1 1 0) and (1 1 1) by the DFT [25] calculations with the generalized gradient approximation (GGA) of Perdew and Wang [26], as implemented in the DMol$^3$ package [27]. The surface was treated with the slab model, in which the neighboring surfaces are separated by 15 Å of vacuum. A supercell of $2 \times 2 \times m$ ($m$ = 3, 4 and 5, layers of substrate) and fine mesh points were chosen in the simulation. It is found that the change of the surface energy is less than 7.0% and 1.0% when the substrate layers change from $m$ = 3 to 4, and

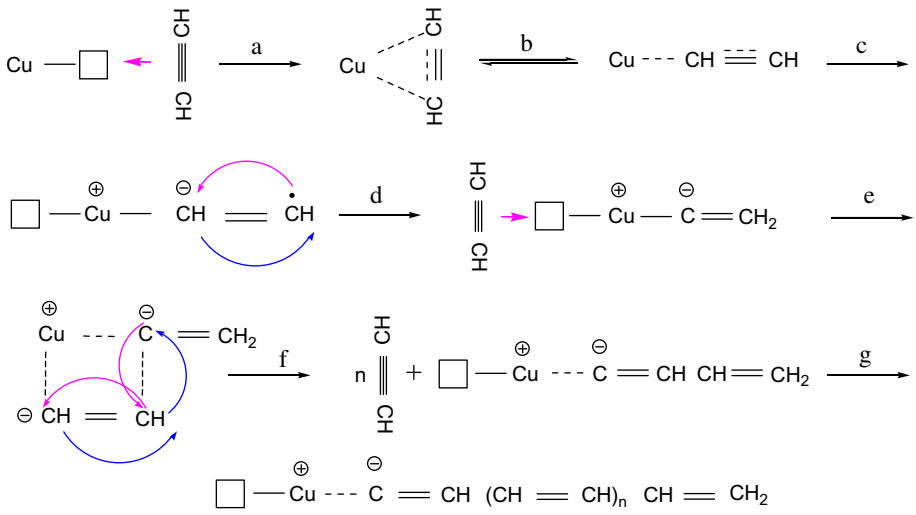


**Fig. 5 – The diagram of the polymerization process of acetylene on copper catalyst (the small squares symbolize the unoccupied orbital of copper).**

from $m = 4$ to 5, respectively. The 4-layer slab model was then selected in the simulation.

The surface energy is given by

$$E_{surf} = \frac{1}{2}\frac{[E_{slab} - N \cdot E_{bulk}]}{A_{hkl}} \quad (1)$$

where $E_{slab}$ is the total energy of an $N$-layer slab, $E_{bulk}$ is the energy per atom in a crystal, $A_{hkl}$ is the area of sectional plane, and $N$ is the number of atoms in the slab supercell. The factor of 1/2 accounts for the two surfaces of the slab. Adsorption energy is evaluated by

$$E_{ad} = E_{acetylene/surf} - E_{acetylene} - E_{surf} \quad (2)$$

where $E_{acetyene}$ and $E_{acetyene/surf}$ are the energies of isolated acetylene and absorbed acetylene-surface system, respectively. The calculated results are summarized in Table 1. It can be found that Cu(1 1 1) plane has the lowest $E_{surf}$, while (1 1 0) has the highest $E_{surf}$ among the three low-index planes of Cu, in agreement with theoretical analysis. The $C_2H_2$ molecule may have several ways to approach the copper surfaces. We examined all the possible modes of interaction between them, and found that five among them were energetically favorable, which are shown in Fig. 6. In all cases, Cu bonds with C atoms and makes $C_2H_2$ bent. Twofold hollow (TFH) adsorption, each C atom bonding with one Cu atom, is found on all the three planes. Two kinds of TFH adsorptions are identified on (1 1 0) where two kinds of Cu–Cu bonds are formed. In addition, fourfold hollow (FFH) adsorption is also found on Cu(1 1 0) where each C atom in $C_2H_2$ bonds two adjacent Cu atoms on (1 1 0).

Table 1 lists the bond lengths of Cu–C, C–C, and the adsorption energies. The TFH adsorption on Cu(1 0 0) gives the largest value of $E_{ad}$ (1.77 eV), which is obviously larger than those of other three TFH adsorptions. It is clear that the adsorptions on (1 0 0) and (1 1 1) are more favorable than that on (1 1 0). The order of the $E_{ad}$ values is also related to the bond lengths of Cu–C and C–C.

Our simulation reveals that the Cu planes have different tendencies to absorb $C_2H_2$ molecules, which reflects the anisotropic nature of Cu crystal. On the other hand, the adsorption of $C_2H_2$ can affect the growth pattern of Cu nanoparticles. Since the surface is partially stabilized by the $C_2H_2$ adsorption, it becomes possible that the crystal keeps growing on this surface and reconstructs into polyhedral structure, as seen in TEM (Fig. 1b) and SEM images (Fig. 2a). Our results and analyses agree well with Qin's speculation [28] that the shape change is caused by the surface reconstruction and the driving force should be the surface energy induced by the acetylene adsorption.

### 3.5. *Forming mechanism of the helical nanofiber*

Considering the relationship between the morphology of the nanofiber and the geometric shape of the catalyst, we make

**Table 1 – $E_{surf}$, $E_{ad}$ and corresponding bond length for different adsorption models.[a].**

| Surface | $E_{surf}$ (J m$^{-1}$) | C–Cu bond length (Å) | C–C bond length (Å) | C–C–H angle (°) | Adsorption site | $E_{ad}$ (eV) |
|---|---|---|---|---|---|---|
| Cu(1 1 1) | 1.32 | 2.043 | 1.377 | 120.02 | Diagonal TFH | 1.23 |
| Cu(1 0 0) | 1.50 | 1.949 | 1.369 | 119.39 | Diagonal TFH | 1.77 |
| Cu(1 1 0) | 1.53 | 2.058 | 1.386 | 118.97 | FFH | 1.00 |
| Cu(1 1 0) | | 1.927 | 1.346 | 119.62 | Side TFH-1 | 1.06 |
| Cu(1 1 0) | | 1.946 | 1.312 | 131.20 | Side TFH-2 | 0.81 |

[a] $E_{surf}$ is the surface energy and $E_{ad}$ is counterpoise-corrected adsorption energies (in eV). C–Cu bond length (in Å) is the distance between C atom of $C_2H_2$ and nearest-adjacent Cu atom. C–C bond length and C–C–H angle belong to acetylene after being adsorbed on Cu faces.

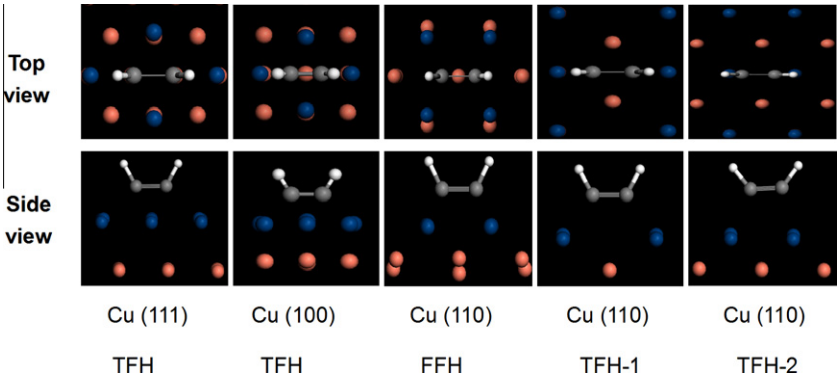


**Fig. 6 – Optimal adsorption sites of acetylene on Cu(1 0 0), (1 1 0) and (1 1 1) surfaces. Cu atoms are denoted by large blue (the first layer) and red (internal layers) balls, C and H atoms of $C_2H_2$ are shown in grey and white, respectively.**

an assay on the catalyst particles obtained from the decomposition of the copper tartrate. According to principles of crystal growth, the surface energy and the growth rate of a facet are inversely proportional to the reticular or lattice density of the respective lattice plane, so faces having low reticular densities grow rapidly and eventually disappear. In other words, high-index faces grow faster than the low-index faces, so that the low-index faces tend to form the surfaces of the crystal. These nanoparticles usually have large surface area leading to high surface energy, which favors particle agglomeration and forms particle of quasi-sphere or ellipsoid.

In Hansen's study [29], the reversible shape changes of copper nanocrystals were observed only in response to the changes in gaseous environment. Wang [30] also observed that a variation in the area ratio of {1 0 0} to {1 1 1} results in a slight difference in particle shape. Our observation confirms that the shape of the catalyst changes during the early stage of the fiber growth (Fig. 2a). Most of the nanofibers change from straight to helical shape after the reaction starts for 5–15 min. Once the polyhedron of the copper particle is formed, the absorbability of acetylene is disparate on different planes, leading to dissimilar rates both in the polymerization and the fiber growth on different planes, so the helical fibers generate. In general, we draw the conclusion that the acetylene adsorption favors the formation of polyhedron copper nanoparticles on which the helical nanofiber forms and grows. With decreasing area ratio of {1 0 0} to {1 1 1}, the copper particles change from sphere to polyhedron (such as octahedron) as shown in Fig. 7.

During the processes of the polymerization and the fiber growth, the concentration of the reactant plays a major role in governing the reaction rate. Since a clear correlation between the nanofiber growth pattern and the adsorption energy is noted, it is reasonable to assume that the adsorption of acetylene on copper surfaces is the rate-control step for the nanofiber growth. Owing to the different adsorption energies (Fig. 6 and Table 1), acetylene is more likely adsorbed on the planes with greater stabilization energy, such as Cu(1 0 0) and Cu(1 1 1), resulting in larger concentration of the reactant on these planes. That means the large rate of polymerization and fast growth for the fibers occur on Cu(1 0 0) and Cu(1 1 1) other than Cu(1 1 0). The acetylene polymerizes at different rates and forms two pieces of helical fibers that grow on the Cu nanoparticle. So the adsorption energy is the driving force

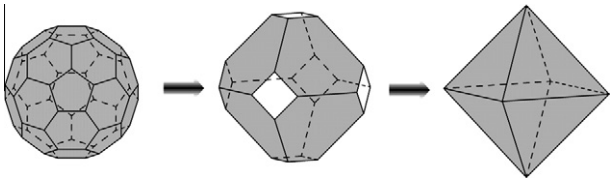

**Fig. 7 – Diagram of the shape changes of a copper particle during the reaction.**

for the gas-induced surface reconstruction, leading to the reshaping of the copper particles. This is the origin of the fiber with helical morphology.

## 4. Conclusion

Copper tartrate decomposes into ellipsoidal copper nanocrystals in various sizes under argon, whereas relatively regular copper polyhedron particles generate under acetylene. The high purity helical nanofibers of organic compounds were synthesized by coordination polymerization of acetylene catalyzed by the generated copper nanopolyhedra. The difference of growth rate induced by the adsorption energy on different surfaces is attributed to the formation of the helical morphology. The new insights on the growth of the novel organic fibers, which have potentials in functional applications, may promote the understanding to the formation mechanism of polymeric helical structures.

## Acknowledgments

This work was financially supported by the National Natural Science Foundation of China (No. 90305003), the Special Research Fund for the Doctoral Program of Higher Education (No. 20060613004), the Ph.D. Programs Foundation (for new teachers) of Education Ministry of China (No. 20070613017) and the Fundamental Research Funds for the Central Universities (No. 2010XS31).

## Appendix A. Supplementary data

Supplementary data associated with this article can be found, in the online version, at doi:10.1016/j.carbon.2010.08.035.

## REFERENCES


[1] Davis WR, Slawson RJ, Rigby GR. An unusual form of carbon. Nature 1953;171(4356):756.
[2] Baker RTK, Harris PS, Terry S. Unique form of filamentous carbon. Nature 1975;253(5486):37–9.
[3] Motojima S, Ueno S, Hattori T, Goto K. Growth of regularly coiled spring-like fibers of $Si_3N_4$ by iron impurity-activated chemical vapor deposition. Appl Phys Lett 1989;54(11):1001–3.
[4] Motojima S, Kawaguchi M, Nozaki K, Iwanaga H. Growth of regularly coiled carbon filaments by Ni catalyzed pyrolysis of acetylene, and their morphology and extension characteristics. Appl Phys Lett 1990;56(4):321–3.
[5] Motojima S, Hasegawa I, Kagiya S, Andoh K, Iwanaga H. Vapor phase preparation of micro-coiled carbon fibers by metal powder catalyzed pyrolysis of acetylene containing a small amount of phosphorus impurity. Carbon 1995;33(8):1167–73.
[6] Yang S, Chen X, Kikuchi N, Motojima S. Catalytic effects of various metal carbides and Ti compounds for the growth of carbon nanocoils (CNCs). Mater Lett 2008;62(10):1462–5.
[7] Yang S, Chen X, Motojima S. Morphology of the growth tip of carbon microcoils/nanocoils. Diam Relat Mater 2004;13(12):2152–5.
[8] Yang S, Chen X, Motojima S, Ichihara M. Morphology and microstructure of spring-like carbon micro-coils/nano-coils prepared by catalytic pyrolysis of acetylene using Fe-containing alloy catalysts. Carbon 2004;43(4):827–34.
[9] Chen X, Motojima S, Iwanga H. Vapor phase preparation of super-elastic carbon micro-coils. J Cryst Growth 2002;237(3):1931–6.
[10] Motojima S, Hoshiya S, Hishikawa Y. Electromagnetic wave absorption properties of carbon microcoils/PMMA composite beads in W bands. Carbon 2003;41(13):2658–60.
[11] Xie G, Wang Z, Cui Z, Shi Y. Ni–Fe–Co–P coatings on coiled carbon nanofibers. Carbon 2005;43(15):3181–3.
[12] Furuya Y, Hashishin T, Iwanaga H, Motojima S, Hishikawa Y. Interaction of hydrogen with carbon coils at low temperature. Carbon 2004;42(2):331–5.
[13] Qin Y, Li H, Zhang Z, Cui Z. Symmetric and helical growth of polyacetylene fibers over a single copper crystal derived from copper tartrate decomposition. Org Lett 2002;4(18):3123–5.
[14] Qin Y, Zhang Z, Cui Z. Helical carbon nanofibers prepared by pyrolysis of acetylene with a catalyst derived from the decomposition of copper tartrate. Carbon 2003;41(15):3072–4.
[15] Wagner RS, Ellis WC. Vapor–liquid–solid mechanism of single crystal growth. Appl Phys Lett 1964;4(5):89–90.
[16] Holstein WL. The roles of ordinary and Soret diffusion in the metal-catalyzed formation of filamentous carbon. J Catal 1995;152(1):42–51.
[17] Shirakawa H, Ikeda S. Infrared spectra of poly(acetylene). Polym J 1971;2(2):231–44.
[18] Tysoe WT, Nyberg GL, Lambert RM. Low temperature catalytic chemistry of the Pd(1 1 1) surface: benzene and ethylene from acetylene. J Chem Soc Chem Commun. 1983;(11):623–5.
[19] Ormerod RM, Lambert RM. Partial oxidation of unsaturated hydrocarbons over Pd(1 1 1): oxygen scavenging of reactive intermediates and the formation of furan from $C_2H_2$ and $C_4H_4$. Catal Lett 1990;6(1):121–30.
[20] Avery NR. Adsorption and reactivity of acetylene on a copper(1 1 0) surface. J Am Chem Soc 1985;107(23):6711–2.
[21] Lomas JR, Baddeley CJ, Tikhov MS, Lambert RM. Ethyne cyclization to benzene over Cu(1 1 0). Langmuir 1995;11(8):3048–53.
[22] Dvorak J, Hrbek J. Adsorbate ordering effects in the trimerization reaction of acetylene on Cu(1 0 0). J Phys Chem B 1998;102(47):9443–50.
[23] Kyriakou G, Kim J, Tikhov MS, Macleod N, Lambert RM. Acetylene coupling on Cu(1 1 1): formation of butadiene, benzene, and cyclooctatetraene. J Phys Chem B 2005;109(21):10952–6.
[24] Qin Y, Jiang X, Cui Z. Low-temperature synthesis of amorphous carbon nanocoils via acetylene coupling on copper nanocrystal surfaces at 468 K: a reaction mechanism analysis. J Phys Chem B 2005;109(46):21749–54.
[25] Hohenberg P, Kohn W. Inhomogeneous electron gas. Phys Rev 1964;136(3B):864–71.
[26] Perdew JP, Wang Y. Accurate and simple analytic representation of the electron-gas correlation energy. Phys Rev B 1992;45(23):13244–9.
[27] Delley B. From molecules to solids with the $DMol^3$ approach. J Chem Phys 2000;113(18):7756–64.
[28] QinY, Zhang Z, Cui Z. Helical carbon nanofibers with a symmetric growth mode. Carbon 2004;42(10):1917–22.
[29] Hansen PL, Wagner JB, Helveg S, Rostrup-Nielsen JR, Clausen BS, Topsøe H. Atom-resolved imaging of dynamic shape changes in supported copper nanocrystals. Science 2002;295(5562):2053–5.
[30] Wang ZL. Transmission electron microscopy of shape-controlled nanocrystals and their assemblies. J Phys Chem B 2000;104(6):1153–75.